ELSEVIER

International Journal of Adhesion & Adhesives 25 (2005) 1–12

International Journal of Adhesion & Adhesives

www.elsevier.com/locate/ijadhadh

Modelling anomalous moisture uptake, swelling and thermal characteristics of a rubber toughened epoxy adhesive

W.K. Loh[a], A.D. Crocombe[a,*], M.M. Abdel Wahab[a], I.A. Ashcroft[b]

[a] *School of Engineering (H5), University of Surrey, Guildford, Surrey GU2 7XH, UK*

[b] *Wolfson School of Mechanical and Manufacturing Engineering, Loughborough University, Loughborough LE11 3TU, UK*

Accepted 6 February 2004

Abstract

Experimental studies have been undertaken to characterise the diffusion, swelling and thermal characteristics of a rubber toughened epoxy adhesive. Gravimetric experiments were carried out for three different thicknesses of bulk adhesive. The bulk adhesives were exposed to 81.5%, 95.8% RH and water immersion, all at 50°C. Dual stage moisture uptake profiles were observed for thin specimens at all levels of exposure. It was found that a dual stage uptake model fits the anomalous uptake response excellently. The swelling of the adhesive was characterised using the same exposure environment. Swelling was slow at low levels of moisture uptake and increased gradually before becoming linear with increasing moisture uptake. The initial slow swelling of the adhesive was attributed to the diffusion of water into the existing free volume. A moisture-dependent swelling coefficient was determined using finite element modelling, where the dual stage uptake model and moisture-dependent mechanical properties of the adhesive were taken into account. The thermal expansion of the bulk adhesive was determined using a bi-material curved beam specimen. The curvature of the beam reduced when it was exposed to a wet environment. This behaviour was successfully modelled using coupled moisture diffusion and stress analysis incorporating the derived moisture-dependent swelling behaviour.

Keywords: A. Epoxy; D. Durability; B. Steels; C. Stress analysis; Swelling and thermal expansion

1. Introduction

An epoxy adhesive is susceptible to moisture attack because it has hydrophilic groups that attract water molecules [1–3]. The hydrophilicity of an epoxy can be caused by the hydroxyl (–OH) groups, these can also form hydrogen bonds with water molecules. Moisture absorbed can act as a plasticiser, solvent or hydrolysis agent for some polymers and adhesives [4]. This contributes to the degradation of the adhesive mechanical properties.

Epoxide adhesives can absorb water up to a maximum of about 10% moisture by mass, depending on the chemical nature and structure, stress state, exposure time, water concentration and temperature. Fickian and non-Fickian moisture uptake characteristics can be exhibited by adhesives. The former generally occurs where the diffusion rate is much quicker than the relaxation rate of the polymer. In such cases, the uptake characteristic shows good agreement with Fick's law [5–7]. Non-Fickian diffusion is generally considered to occur when the relaxation of the polymer influences the uptake behaviour. Such responses are conventionally divided into two groups. One is known as Class II (Class I being Fickian diffusion) and generally occurs when the relaxation rate, rather than the diffusion rate, controls the uptake. In these cases, the uptake often increases linearly with time. The other group is termed anomalous uptake and generally occurs when diffusion and relaxation have comparable rates. A common moisture uptake profile within this group is dual stage uptake [8–10]. This exhibits initial Fickian diffusion uptake followed by a reduced uptake rate, finally reaching a saturation level at extended exposure times. On occasion, leaching behaviour may be observed when loss of the adhesive occurs following high-temperature exposure [8] or incomplete curing [11]. An additional increase of mass uptake after initial Fickian diffusion can be attributed to

*Corresponding author. Tel.: +44-0-1483-689-194; fax: +44-0-1483-306-039.

E-mail address: a.crocombe@surrey.ac.uk (A.D. Crocombe).

0143-7496/$ - see front matter © 2004 Elsevier Ltd. All rights reserved.
doi:10.1016/j.ijadhadh.2004.02.002

increased swelling and relaxation, particularly at high temperatures [6]. Several diffusion models have been proposed to predict the anomalous moisture uptake. Cai and Weitsman [12], Gurtin and Yatomi [13], and Carter et al. [14] have used different nonlinear diffusion parameters to model anomalous diffusion in polymeric and composite materials. As with Fickian diffusion, these anomalous diffusion models are not universally applicable to all systems.

The swelling of an adhesive after exposure to moisture also plays an important role in bonded joint durability. Depending on the exposure environment and type of adhesive, the volumetric expansion can reach 10%. Adamson [15] recorded about 4% and 5% swelling of an epoxy resin when exposed to water at 40°C and 74°C, respectively. El-Sa'ad et al. [16] recorded about 1% and 10% swelling of a cured rubber filled epoxy adhesive when exposed to 23°C and 60°C, respectively in water. Chang et al. [17] found that, for the adhesive considered, the swelling showed a linear relationship with the relative humidity. The swelling of adhesives generally increases with moisture content and exposure temperature. A significant amount of adhesive swelling can induce stresses and thus play an important role in joint durability. Its effect should be included in durability modelling of adhesive joints.

The curing process of adhesives and thermal cycling environments can induce thermal stress and strain, as well as altering the mechanical properties, when bonded to stiff elastic substrates. This residual stress and strain can lead to damage and debonding and thus affect the durability of adhesively bonded joints. Dillard et al. [18] concluded that the failure of bi-material systems can occur under a cyclic temperature environment. Although their work focused on the thermal cycling, they stated that the effect of absorption and desorption cycles of moisture could produce the same effects. Nakano et al. [19] showed the development of stress concentrations, under thermal loading, at the periphery of holes or fillers in an adhesive using both an analytical method and a photoelastic experiment. They concluded that both the stress concentration at the hole or filler periphery and the stress singularity at the edge of the interface play an important role in determining the joint strength.

The main objective of the work presented here is to characterise the moisture absorption, swelling and thermal characteristics of an adhesive for subsequent durability modelling. Bulk adhesive specimens were exposed to a range of ageing environments to study the moisture diffusion and swelling characteristics. A dual stage moisture transport model is proposed to simulate the observed uptake characteristics of the bulk adhesive. This dual stage uptake can be easily modelled using finite element (FE) analysis. The effect of moisture on the mechanical properties of the adhesive was investigated using tensile tests and these data were used during subsequent FE modelling. A bi-material curved beam was used to determine the coefficient of thermal expansion (CTE) and the combined effect of thermal expansion and moisture swelling of the adhesive. The effects of swelling on the reduction of curvature of the bi-material curved beams were investigated experimentally and numerically. Coupled diffusion-mechanical FE analyses were used to model (a) the dual stage diffusion, (b) the swelling, and (c) the thermal effects of the adhesive.

2. Adhesive and ageing environment details

AV119 (Araldite 2007) was chosen for the study. This is a one-part rubber toughened epoxy adhesive produced by Vantico. It is a multi-purpose, heat curing thixotropic (no flow during cure) paste adhesive of high strength and fracture energy. AV119 was cured at an oven temperature of 120°C for 2 h. Three moisture environments, 81.2% RH, 95.8% RH and water immersion, were used, all at 50°C. Saturated salt solutions KCl and K_2SO_4 were used to generate the two relative humidities, respectively, while distilled water was used for the water immersion. The conditioning chambers were placed in an oven at 50°C and were monitored closely with a digital hygrometer to ensure that the desired environment had been achieved.

3. Gravimetric experiments

The rate of degradation of adhesively bonded structures is governed by the moisture diffusion performance. It is important that the moisture diffusion is modelled correctly in order to predict the residual strength of an adhesively bonded structure accurately. The moisture uptake performance of AV119 was determined using thin film bulk adhesive specimens. Three thicknesses of bulk adhesive film (0.4, 0.8 and 2.0 mm) were used. In order to combine gravimetric and tensile testing, "dog-bone" specimens were made and exposed from the 0.4 and 0.8 mm films. The specimen sizes resulted in a suitably large surface area to thickness ratio, ensuring that the diffusion process was essentially one-dimensional. There are three basic stages in making the bulk tensile "dog-bone" specimen. First of all, the adhesive was cast into small individual sheets of bulk adhesive by sandwiching the adhesive paste between two steel plates covered with release film. The thickness of the bulk adhesive was controlled using spacers. Then, the adhesive was cured. This individual bulk adhesive film was machined into the required "dog-bone" profile shown in Fig. 1 on a CNC machine with no lubrication. Lastly, the specimens were finely

abraded with fine abrasive paper to bring them to their correct thickness, removing approximately 0.5 mm. The completed "dog-bone" specimens were kept in a dry desiccator for a minimum of 10 days prior to exposure. Then, each of the specimens were exposed to the appropriate ageing environment. Removal of the specimen for weighing was carried out such that the disturbance of the equilibrium environment in the chamber was minimised. The surface of the specimen was wiped dry using analytical grade tissue paper before weighing using a Mettler M5 analytical microbalance. Data were read to 0.01 mg although this is well above the accuracy of the balance which is 0.002 mg. The specimen was then returned to the chamber as soon as possible. The initial weight of the dry bulk specimens, M_0, was measured first. The subsequent weighing of the exposed bulk specimens, M_t, was undertaken periodically with the exposure time recorded. The moisture content (mwt_t) can be calculated at each exposure and is expressed in terms of percentage throughout.

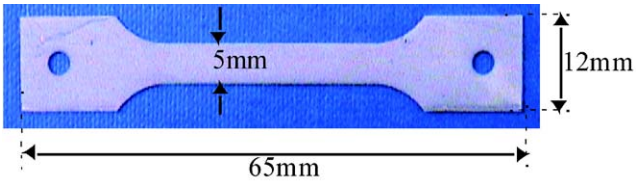

Fig. 1. "Dog-bone" specimen for tensile test (all dimensions are in mm).

The percentage moisture content as a function of $\sqrt{t/l^2}$ is shown in Figs. 2–4 for increasing film thickness; where t is the time of exposure and l is the initial half thickness of the bulk adhesive film. It can be observed that the rate of mass uptake was greater at the beginning of the exposure and gradually diminished as the moisture content approached the saturation level in all cases. The final recorded moisture level, which is at or very close to equilibrium, has been taken as the saturation value. The effect of the ageing environment on this saturation level (mwt_∞) is clearly observed for all different thicknesses as listed in Table 1. The saturation level increased with relative humidity, as noted elsewhere [6,20,21]. Furthermore, the results also show that there was a large increase of saturation level between 95% RH and immersion in water. The saturation level was not very different between thicknesses of 0.4 and 0.8 mm but the mass gain of the 2 mm thick film specimens was about 20% higher than the corresponding thinner specimens. This could be due to differences in the chemical structure between the thin and thick films. These might include voids, residual stresses, boundary layers, etc.

3.1. Fickian diffusion

Fickian diffusion is commonly used to model the diffusion behaviour of moisture into adhesive polymers [5]. Considering the one-dimensional case, the analytical solution, giving the temporal and spatial moisture concentration (c) at time t and distance x from the

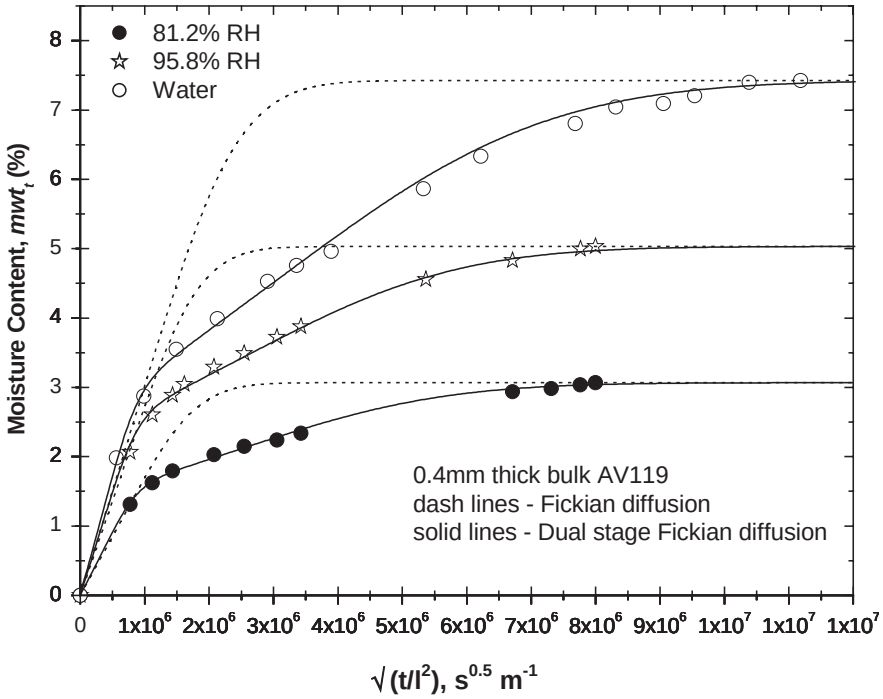

Fig. 2. Experimental, standard Fickian and dual stage Fickian diffusion data for 0.4 mm thick specimens for the range of ageing environments.

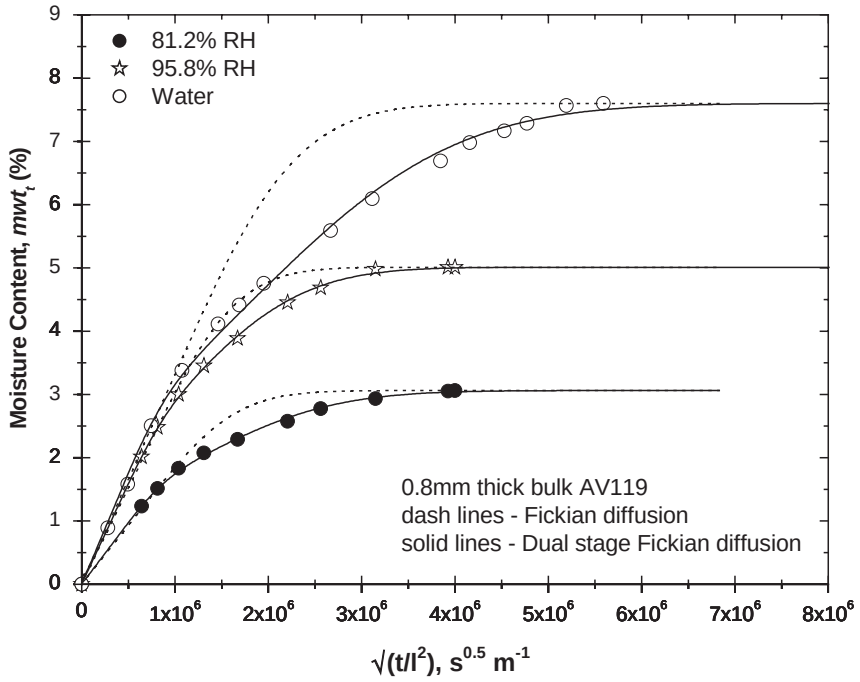

Fig. 3. Experimental, standard Fickian and dual stage Fickian diffusion data for 0.8 mm thick specimens for the range of ageing environments.

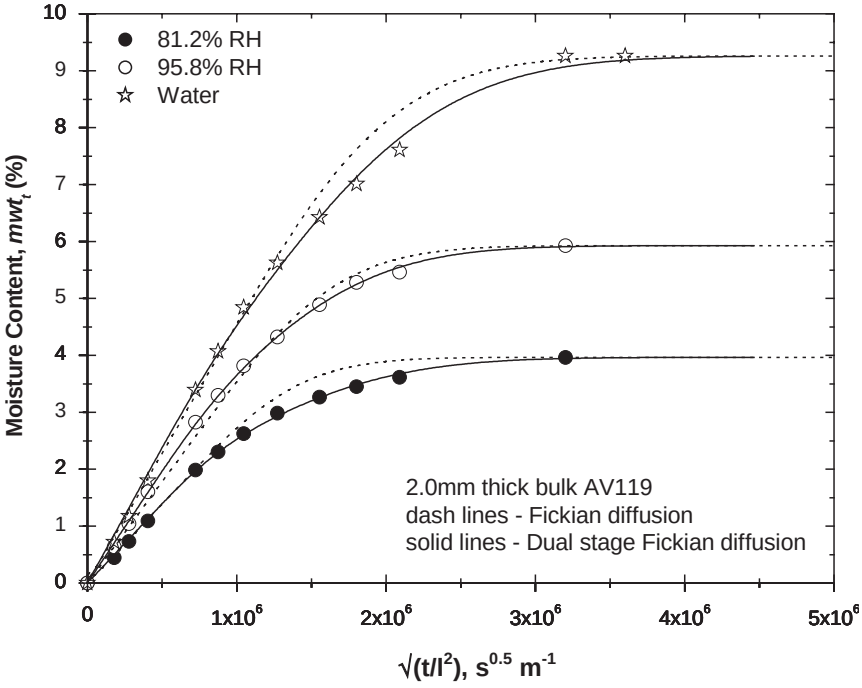

Fig. 4. Experimental, standard Fickian and dual stage Fickian diffusion data for 2.0 mm thick specimens for the range of ageing environments.

mid-plane, is shown in Eq. (1). Here c_∞ is the maximum equilibrium moisture concentration, D is the Fickian diffusion coefficient and l is the half thickness of the bulk adhesive film. As it is experimentally difficult to measure moisture concentration at a point in the adhesive, the expression is integrated giving the fractional mass uptake of the specimen ($\mathrm{mwt}_t/\mathrm{mwt}_\infty$) as a function of time, in Eq. (2). This equation can be used to predict the moisture uptake. Eq. (3) is a simplified form of Eq. (2) that has been used to determine the Fickian diffusion coefficient. This equation is a close approximation to Eq. (3) but only for short exposure times

Table 1
Moisture saturation levels and Fickian diffusion coefficients for different ageing environments and thicknesses at 50°C

Ageing environment	Thickness					
	0.4 mm		0.8 mm		2.0 mm	
	mwt_∞ (%)	D (m^2/s)	mwt_∞ (%)	D (m^2/s)	mwt_∞ (%)	D (m^2/s)
81.2% RH	3.07	24×10^{-14}	3.06	29×10^{-14}	3.96	38.5×10^{-14}
95.8% RH	4.99	24×10^{-14}	5.01	29×10^{-14}	5.93	28.3×10^{-14}
Water	7.43	13×10^{-14}	7.60	15×10^{-14}	9.26	19.0×10^{-14}

where the mass uptake is up to about 60% of the equilibrium value.

$$\frac{c}{c_\infty}=1-\frac{4}{\pi}\sum_{n=0}^{\infty}\frac{(-1)^n}{(2n+1)}\exp\left[\frac{-D(2n+1)^2\pi^2t}{4l^2}\right]\times\cos\left(\frac{(2n+1)\pi x}{2l}\right), \quad (1)$$

$$\frac{mwt_t}{mwt_\infty}=1-\frac{8}{\pi^2}\sum_{n=0}^{\infty}\frac{1}{(2n+1)^2}\exp\left[\frac{-D(2n+1)^2\pi^2t}{4l^2}\right], \quad (2)$$

$$\frac{mwt_t}{mwt_\infty}=\frac{2}{l}\sqrt{\frac{Dt}{\pi}}. \quad (3)$$

Initially, the experimental data are fitted with the Fickian diffusion model. The Fickian diffusion coefficients for each level of exposure and thickness were obtained as shown in Table 1 using Eq. (2). These data were then used in conjunction with the equilibrium mass uptake values and Eq. (2) to obtain a predicted uptake curve. These predicted results (dashed lines) are shown in Figs. 2–4. From these figures, it can be seen that the Fickian diffusion model with constant diffusion coefficient failed to fully reproduce the experimental uptake curves in all cases except the 2.0 mm thick adhesive film, where reasonable agreement is found. Fickian diffusion over-predicts the experimental results after the initial, linear uptake phase. This observation has been reported elsewhere [8,9]. These results suggest that the uptake for thicker specimens or for longer diffusion paths can be modelled using Fickian diffusion, whilst the thinner specimens need an anomalous (non-Fickian) uptake model to simulate their response. In order to model the moisture uptake response of the thin specimens, a dual stage uptake model was developed and is discussed below.

3.2. Dual stage uptake

The dual stage uptake model developed in this work consists of two Fickian diffusion models in parallel. Both of the Fickian diffusion models use Eq. (2) with separate diffusion coefficient (D_1 and D_2) and saturation levels ($mwt_{1\infty}$ and $mwt_{2\infty}$), respectively. The sum of each saturation level gives the total saturation.

Table 2
Uptake parameters for dual stage Fickian diffusion at 50°C

Thickness	Ageing environment	D_1 (m^2/s)	D_2 (m^2/s)	$mwt_{1\infty}$ (%)
0.4 mm	81.2% RH	100.0×10^{-14}	2.5×10^{-14}	1.35
	95.8% RH	100.0×10^{-14}	2.3×10^{-14}	2.21
	Water	100.0×10^{-14}	1.5×10^{-14}	2.45
0.8 mm	81.2% RH	100.0×10^{-14}	11.0×10^{-14}	1.07
	95.8% RH	100.0×10^{-14}	14.0×10^{-14}	1.50
	Water	100.0×10^{-14}	5.0×10^{-14}	1.82
2 mm	81.2% RH	100.0×10^{-14}	18.5×10^{-14}	1.35
	95.8% RH	100.0×10^{-14}	21.0×10^{-14}	1.35
	Water	100.0×10^{-14}	14.0×10^{-14}	1.20

A least mean-squares approach together with a univariant search method was developed using MATLAB programming to obtain the best fit diffusion parameters (D_1, D_2 and $mwt_{1\infty}$) for the experimental results ($mwt_{2\infty}$ is found as $mwt_\infty - mwt_{1\infty}$). The experimental results were first converted into polynomial functions which were needed to provide reference curves for the least-square fit procedure. It was found from the fitting process that D_1 was within the range of 90–110×10^{-14} m^2/s for all ageing environments and thicknesses considered. This could indicate that the initial mass uptake of the adhesive is essentially independent of the relative humidity and thickness. For convenience, D_1 was set as 100×10^{-14} m^2/s and D_2 and $mwt_{1\infty}$ were obtained by running the search program again. The diffusion parameters from these best fitting processes are listed in Table 2. There does not appear to be a consistent trend in D_2. However, the predicted dual stage results for each moisture uptake experiment (solid lines) are shown in Figs. 2–4 and the results show the good correlation, over the entire data range, between the "best fit" and the experimental data.

Plotting the film mid-plane concentration ($x=0$) against the fractional mass uptake using Eqs. (1) and (2) (Fickian diffusion) gives a unique curve, shown as a solid bold line in Fig. 5 for all film thicknesses. This unique curve shows that the mid-plane moisture concentration is initially zero and remains so for some time and so lags behind the fractional mass uptake at the

beginning of exposure period. This is due to the time required for the moisture to reach the mid-plane. After 0.35 fractional mass uptake, the mid-plane concentration increases linearly until it reaches the saturation level ($c_\infty = \mathrm{mwt}_\infty$). The same curves were determined using the dual stage uptake model. The plot of the film mid-plane moisture concentration against the fractional mass uptake for all three thicknesses at 81.2% RH are also shown in Fig. 5. The figure shows that the 2 mm thick specimen behaves more like a Fickian diffusion response; whereas the thinnest specimen (0.4 mm), deviates from this standard response. A reason for this could be that the moisture diffusion into a thin specimen occurs in a much shorter time period than a thicker specimen and occupies the existing voids in the material, which leads to a mass gain of $\mathrm{mwt}_{1\infty}$. The second stage uptake becomes apparent when volumetric swelling occurs and voids enlarge slowly. This generally results in an additional amount of mass gained ($\mathrm{mwt}_{2\infty}$) at a lower diffusion rate. This argument is supported later by the swelling behaviour where it will be seen that swelling is low at the beginning and then increases after the mass gain approaches $\mathrm{mwt}_{1\infty}$. The dual stage response is less apparent as the film thickness increases because these specimens swell less readily as a result of the longer diffusion path. Alternatively the chemical nature and structure of the cured thin and thick films might be different.

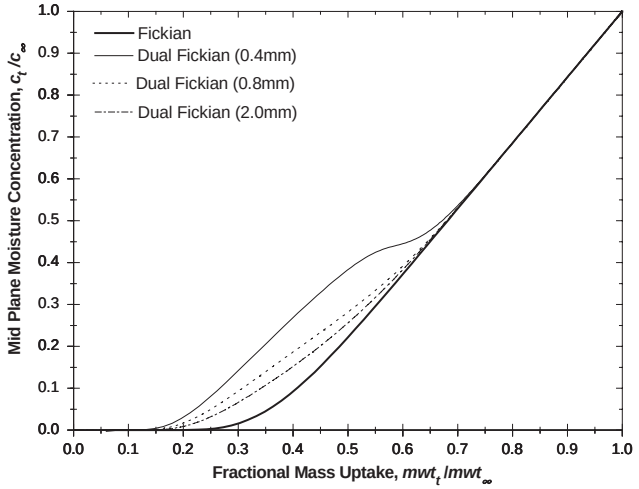

Fig. 5. The variation of mid-plane moisture concentration with fractional mass uptake for different thicknesses when exposed to 81.2% RH at 50°C.

3.3. Modelling moisture diffusion

The FE method has the capability of analysing a transient moisture diffusion response. Based on the results obtained from the gravimetric experiments in the previous section, the experimental moisture uptake data were modelled excellently using the dual stage uptake model. For subsequent use when analysing more complex diffusion paths in adhesively bonded structures, this dual stage model needs to be implemented within an FE framework. This can be done by combining the FE nodal moisture concentrations from two separate Fickian diffusion analyses. A general FE model was generated using four noded elements to model the dual stage diffusion analyses as shown in Fig. 6. It should be noted that the film thickness is in the horizontal direction and the resulting moisture profile will be one-dimensional in this direction. The diffusion coefficients, D_1 and D_2 listed in Table 2 for 0.4 mm thick bulk adhesive films exposed to 81.2% RH/50°C were used to describe the material properties for the analyses considered here. FE analysis is undertaken in terms of the normalised moisture concentration c/c_∞. The boundary condition applied to the left- and right-hand edges of the model was $c_{1\infty}/c_\infty$ and $c_{2\infty}/c_\infty$ for the first and second stages, respectively. Here $c_{1\infty}$ and $c_{2\infty}$ are equivalent to $\mathrm{mwt}_{1\infty}$ and $\mathrm{mwt}_{2\infty}$, respectively, and are normalised against the maximum moisture absorption c_∞, which is taken to be 7.60%. These boundaries were assumed instantaneously saturated at the exposed edges. Each of the individual Fickian diffusion analyses were solved incrementally for the specified period of time and then combined to give the dual stage diffusion response. The FE solution obtained was validated using the analytical solutions. It was found that both solutions showed good agreement in standard Fickian diffusion as well as dual stage uptake, as shown in Fig. 7.

4. Moisture-dependent constitutive properties

Moisture-dependent mechanical properties of environmentally aged bulk AV119 were determined using uniaxial tension tests. Two thicknesses of bulk adhesive

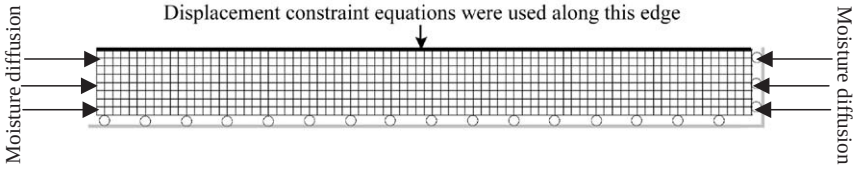

Fig. 6. FE model for moisture diffusion and swelling analysis.

film (0.4 and 0.8 mm) were considered here. The "dog-bone" specimens, shown in Fig. 1, were exposed to the aging environments discussed above for a range of exposure times. After exposure, the specimens were tested using an Instron 5500 test machine with a 5 kN load cell. Testing was conducted in an ambient laboratory environment using a constant crosshead speed of 0.5 mm/min. Strain was measured using an extensometer. The modulus was determined automatically using the accompanying Merlin software, which implements the ISO 527 standard.

Typical uniaxial stress–strain curves for the 0.8 mm thick adhesive for different levels of moisture content are shown in Fig. 8. It should be noted that these moisture contents are averaged values as intermediate moisture contents are obtained by withdrawing a specimen from exposure before saturation. In these cases the moisture profiles will not be uniform across the film thickness. From the figure, it is apparent that the elastic modulus and ultimate tensile stress reduced as moisture content increased. A corresponding trend in strain to failure is not as apparent. This is possibly due to premature failure at some stress raiser that prevents the true failure strain from being reached. Key moisture-dependent mechanical properties are shown in Fig. 9 as a function of fractional mass uptake, based on a saturation value of 7.60%. In all tests, the 0.4 and 0.8 mm specimens gave consistent results. Looking at the elastic modulus, both 0.8 and 0.4 mm specimens show a steady reduction of 38% in elastic modulus over the range of moisture considered. The reduction of elastic modulus could be due to plasticisation by the absorbed water and the disruption of hydrogen bonds between the molecular chains in the adhesive. The difference in elastic modulus between 0.8 and 0.4 mm specimens is negligible. These form the moisture-dependent constitutive properties used in subsequent durability modelling. As well as changes in mechanical properties, bleaching of colour of AV119 from beige to white also indicated the degradation. It is interesting to note that the fractional mass uptakes have been obtained by exposure to a range of environments. Thus a given mass uptake can be achieved at a number of exposure times. The data however appears to be a function only of mass uptake and not the time of exposure. This has important implications for later modelling work.

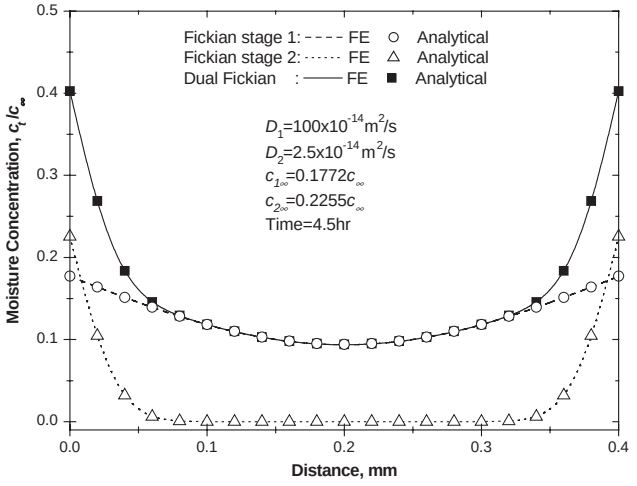

Fig. 7. Moisture concentration profiles of 0.4 mm thick bulk adhesive exposed to 81.2% RH at 50°C. The results obtained from both analytical (Eq. (1)) and FE methods are identical.

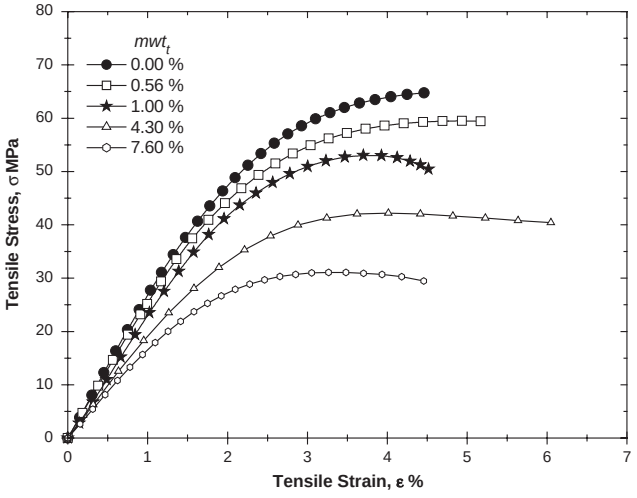

Fig. 8. Typical moisture-dependent stress–strain curves for 0.8 mm thick adhesive "dog-bone" specimens.

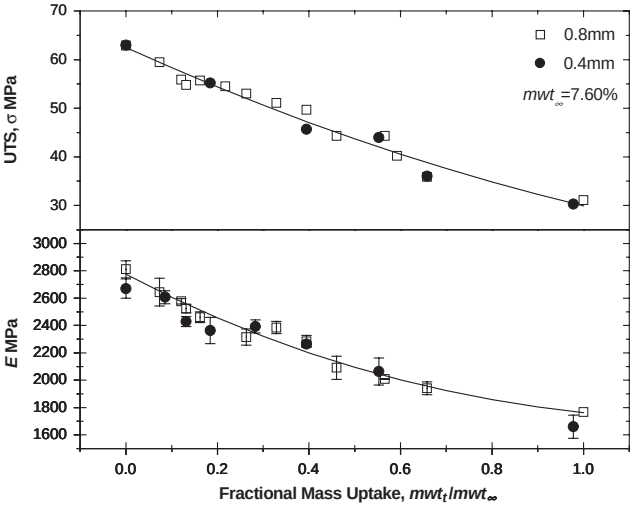

Fig. 9. Moisture-dependent constitutive properties of the adhesive.

5. Swelling

Swelling of the adhesive can have an important effect on adhesive joint durability as it can induce significant

strains. The water molecules occupy positions between the polymer molecules, forcing these macro-molecules apart such that swelling occurs. ''Dog-bone'' specimens with a thickness of 0.4 mm were used to determine the swelling effect. The thin specimen gives a more uniform moisture profile and state of swelling. The specimens were exposed at 50°C 81.5% RH, 95.8% RH and fully immersed in water as described earlier. By assuming that the adhesive has the same swelling strain in all dimensions, a one-dimensional swelling strain was measured using a non-contacting projector microscope.

Two pairs of gauge lengths were lightly marked on the surface of the specimen using a sharp knife. The distance of each gauge length was measured using a projector microscope. This measurement was done before and during exposure to moisture. The exposed specimens were allowed approximately 10 min to cool down from 50°C to a room temperature of 23°C in order to remove the effect of thermal expansion before measuring. The moisture uptake of the specimens was also recorded using the gravimetric approach discussed earlier. The specimen was returned to the ageing environment and the cycle repeated. The ratio of extension measured to the original gauge length gives the swelling strain (ε_{sw}).

The results from the experiments are shown in Fig. 10. Each of the data points shown is the average strain value obtained from the two gauge lengths. The standard deviation of each data point was very small. The swelling of the adhesive starts off slowly at a low moisture concentration and then swelling picks up and becomes linear beyond a fractional mass uptake of 0.2. It is suggested that the slow swelling at the beginning is due to the diffused moisture filling up the existing voids and so only limited volumetric displacement occurs. The swelling becomes more apparent when increased moisture causes increased pressure and possibly also interacts with the polymer. The swelling stopped when the specimen reached its saturation level. The maximum swelling achieved is nearly 2% when submerged in water at 50°C. Swelling strains of 3% have been recorded elsewhere [22], where the same adhesive was exposed at 60°C. It is not surprising that more extensive swelling and plasticisation occur at this higher temperature, which results in more space for moisture transport in the adhesive that, in turn, causes more volumetric displacement.

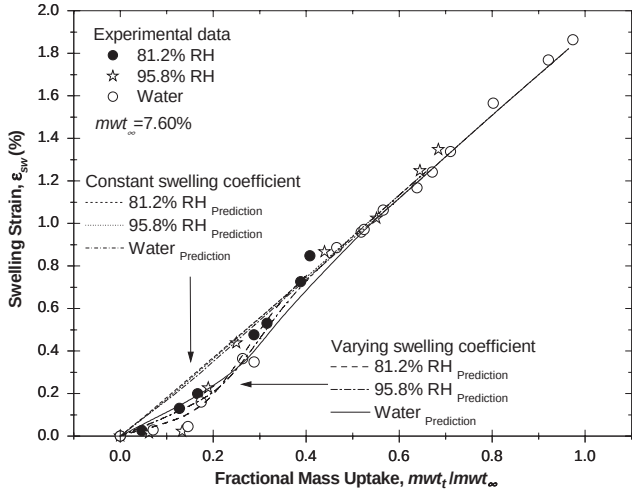

Fig. 10. Experimental and predicted swelling strains as a function of moisture content.

The swelling strains showed excellent agreement even though they were exposed to different ageing environments and exposure times. This leads to the conclusion that the swelling is only a function of the amount of moisture and does not show any significant dependence on the relative humidity in which they were exposed. A similar conclusion was drawn above in reference to the moisture-dependent mechanical properties of the adhesive. The maximum swelling recorded for 81.2% RH, 95.8% RH and submerged in water are 0.9%, 1.4% and 1.89%, respectively. No further swelling was recorded after they reached their respective saturation levels.

The swelling coefficient for AV119 was determined using FE analysis in an iterative manner. These analyses used the diffusion and mechanical properties data determined above. Following the moisture diffusion modelling work, the swelling analysis was implemented using the same FE model, shown in Fig. 6, with some modification to the model files. The type of element has been changed to a plane stress element. The model was fixed at the bottom and right edges and was allowed to swell to the left and top. Displacement constraint equations were used to ensure the top edge displaces uniformly in the vertical direction. A moisture-dependent elastic modulus was included together with an estimated swelling coefficient (α_{sw}). This α_{sw} is analogous to the CTE. The moisture concentration profile obtained from the earlier dual stage moisture uptake analysis was extracted from the results file. This was then read into the swelling analysis initially as a predefined field variable that determined the varying mechanical property across the adhesive layer and secondly as a change in ''temperature'' (moisture concentration).

A constant value for the swelling coefficient of 1.89×10^{-2} was used initially to predict the experimental results at a range exposure times. This was taken directly from the gradient of the later part of experimental data in Fig. 10. It was found that a constant swelling coefficient did not predict the observed experimental data well, particularly at low fractional mass uptakes as shown in Fig. 10. This suggests that the swelling coefficient of the adhesive is also dependent on the moisture concentration. After a few trials, the moisture-dependent swelling coefficient shown in Fig. 11 was found to give a satisfactory prediction over the entire range of all ageing environments, as shown in Fig. 10. The low swelling coefficient used at lower moisture

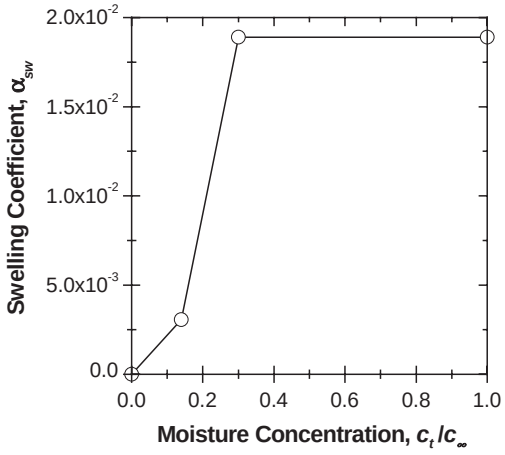

Fig. 11. Calibrated moisture-dependent swelling coefficient of AV119.

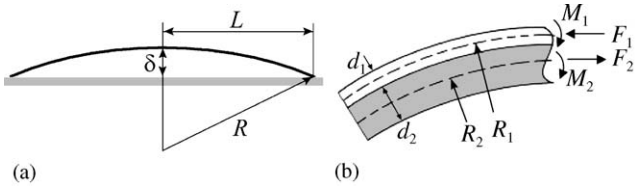

Fig. 12. (a) The deflection, and (b) sectional view of the bi-material curved beam.

concentrations is due to the fact that moisture ingresses into the existing space in the polymer network without causing much swelling. As moisture uptake increases, the degradation rate increases and subsequently enlarges the voids for more swelling.

6. Thermal coefficient characterisation

Characterisation of the CTE was carried out using a bi-material curved beam. When two dissimilar materials are firmly attached (forming a bi-material strip) and experience a drop in temperature ΔT, the strip curves as shown in Fig. 12(a), depending on the CTEs of the materials. If the CTE of one material is known, it is possible to determine the CTE of the other material. The solution to this problem begins by equating the strains at the interface from both strips in terms of their respective tensions, moments and thermal strains, Eq. (4)

$$\frac{F_2}{A_2E_2}+\frac{M_2d_2}{2E_2I_2}+\alpha_2\,\Delta T=-\frac{F_1}{A_1E_1}-\frac{M_1d_1}{2E_1I_1}+\alpha_1\,\Delta T. \quad (4)$$

Here E_1 and E_2 are the elastic moduli and, α_1 and α_2 are CTEs of these materials; F_1 and F_2 are the tensile and compressive forces normal to the cross section, M_1 and M_2 are the moments which must balance the internal forces as indicated in Fig. 12(b). I_1 and I_2 are the cross section second moment of area. This can be simplified by recognising that F_1 is equal and opposite to F_2, by applying equilibrium of moments and by assuming that the radius of curvature are the same for both strips, resulting in Eq. (5)

$$\alpha_2=\alpha_1-\frac{1}{R\,\Delta T}\left[\frac{2(E_1I_1+E_2I_2)}{(d_1+d_2)}\left(\frac{1}{d_1E_1}+\frac{1}{d_2E_2}\right)+\frac{(d_1+d_2)}{2}\right]. \quad (5)$$

Finally, *when the deflection* (δ) *is much smaller than the length* (L), the radius of curvature (R) can be approximated using Eq. (6)

$$R=\frac{L^2}{2\delta}. \quad (6)$$

A bi-material curved beam was produced by curing a layer of adhesive on a thin steel sheet of known dimension. A preliminary study using a two-dimensional FE model was undertaken to determine the thickness of the adhesive layer required to give significant deflection for practical measurement. In this analysis, values of CTE were assumed to be $11.1\times10^{-6\circ}C^{-1}$ and $36.2\times10^{-6\circ}C^{-1}$ for the steel and epoxy adhesive, respectively. The elastic modulus of the steel and AV119 are taken to be 207 GPa and 2774 MPa, respectively. A drop of temperature of 100°C was applied. The steel sheet thickness was set at 0.2 mm whereas the thickness of the adhesive was allowed to vary. It was found that a range of adhesive thicknesses between 0.2 and 2 mm gave sufficient deflection.

A steel strip of $120\times20\,mm^2$ was cut from a larger piece of steel sheet. The steel surface was evenly grit blasted with white alumina grit size of 180/220, cleaned twice by soaking with acetone in an ultrasonic bath for 2 min each time and then drying at room temperature. Initially, a 0.2 mm adhesive layer was cast but the end product showed uneven adhesive thickness, was too flexible for handling and even flattened under its own weight. When a 1 mm thick adhesive layer was cast, the curved beam was more rigid and robust for manual handling. When this bi-material specimen is exposed, moisture only enters the adhesive from one side and thus the diffusion characteristics for the 2 mm thick bulk adhesive film (where moisture enters from both sides) will be used in later modelling work. After curing, the strip was carefully detached from the clamp. The spacers at each end were carefully cut out using a saw. The final length of the curved beam was 100 mm. Any additional adhesive extending beyond the steel strip was carefully removed using a file. The end product of the bi-material curved beam is shown in Fig. 13. The beam responded elastically when pressure was applied and released at the middle of the beam. Two nominally identical curved beams were manufactured for this experiment.

The deflection of the curved beam was measured using a Linear Variable Differential Transformer (LVDT) over a range of elevated temperatures T_0. The

LVDT was slightly modified for this application by removing the spring in the spring-loaded core. The core itself is very light and did not cause any noticeable reduction of deflection of the curved beam. From calibration with slip gauges, it was found that the LVDT was insensitive to temperature over the range used. The measured displacement is shown in Fig. 14. It was observed that the deflection reduced linearly as the temperature increased. The reference temperature T_R is the temperature at which the beam lay flat, with no deflection ($\delta = 0$). This corresponds to the strains across both materials being equal and is the temperature at which, on cooling, the thermal strains are locked into the system. T_R was evaluated by extrapolating the data until it intersected the x-axis. T_R is likely to be a little lower than the glass transition temperature T_g as it is likely that some "flow" will still occur in this region. For this adhesive system, T_g has been measured as 110°C, which, as expected, is a little higher that the T_R value of 90°C from Fig. 14. The effective change of temperature ΔT experienced by the curved beam for residual strain calculation was the difference $(T_0 - T_R)$ and not the difference of $(T_0 - T_c)$ where T_c is the curing temperature. This is because the adhesive becomes rubbery at temperatures above T_R and hence thermal mismatch above this temperature is accommodated by flow in the adhesive. The CTE of AV119 was evaluated at different temperatures as shown in Fig. 15, using Eq. (5) neglecting the effect of temperature on the elastic modulus of the adhesive. This is not a reasonable assumption when the temperature is higher than about 30°C below T_g. As the T_g for this adhesive is around 110°C, this is a reasonable approximation for most of the data shown in Fig 15 and the rise in CTE at the higher temperatures could result from not including the reduction in adhesive modulus. Hence, the CTE obtained at lower temperatures are more accurate. The average value of CTE of $6.12 \times 10^{-5}\,°C^{-1}$ at 23°C was verified using FE analysis to predict the experimental results as shown in Fig. 14. Good correlation is found between the analytical solution and FEA and the values for the CTE are reasonable for a toughened epoxy. This bi-material curved beam seems to be successful in determining the CTE of the AV119. The deformation plots of the curved beam at different changes of temperature are shown in Fig. 16.

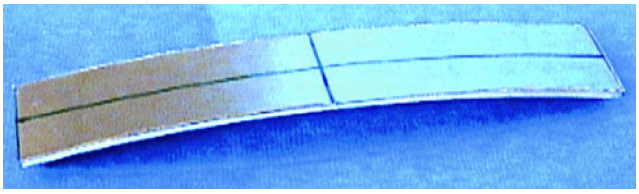

Fig. 13. Bi-material curved beam (100 mm length and 20 mm wide).

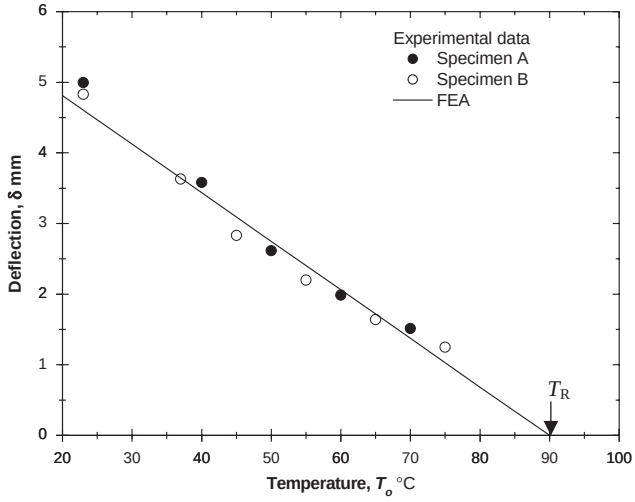

Fig. 14. Deflection measured experimentally as a function of temperature. The FEA results show good prediction of the reduction of deflection as temperature increases.

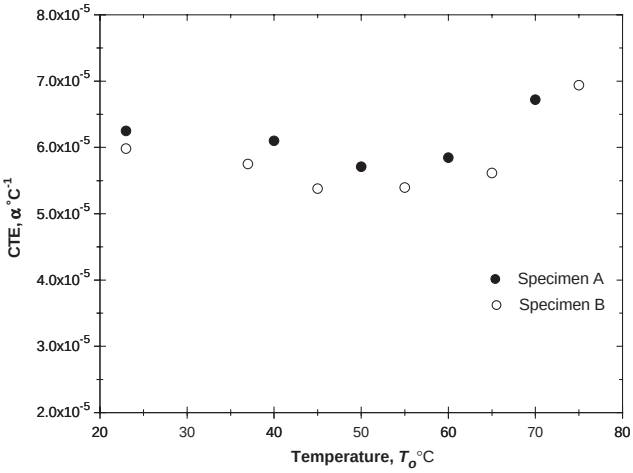

Fig. 15. CTE as a function of temperature.

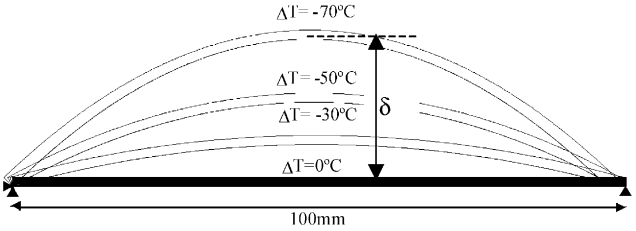

Fig. 16. Deformation plots of bi-material curved beam for a range of temperature drops obtained from FE analysis.

7. Combined effect of thermal and swelling

The bi-material curved beams manufactured above were also used to measure the reduction of deflection when exposed to an ageing environment. The moisture

diffused through the open face of the adhesive. It was expected that the swelling of the adhesive would counter the thermal stress and reduce the curvature of the beam. The reduced curvature measured can be compared with the FE modelling for validation of thermal expansion coefficient and swelling coefficient of the adhesive obtained separately in earlier sections. It also provides an assessment of the methodology used for modelling both thermal and swelling strains simultaneously.

Before exposure to the moist environment, the bi-material curve beam was coated with two layers of anti-rust primer paint on the steel sheet and around the perimeter interface to protect the steel from corrosion in the moist environment (95% RH/50°C). This also restricts the moisture diffusing along the interface and edge delamination. It is believed that this thin layer of primer paint had a negligible effect on the deflection of the bi-material strip. During exposure, the curved beams were taken out from the chamber periodically to measure the deflection, δ. The measurement of deflection was taken when the strip deflection had stabilised, indicating that the specimen had cooled to ambient temperature.

The results are shown in Fig. 17. The two specimens (A and B) show the same response of an initial reduction of deflection from about 4.5 to 1.5 mm when they were exposed for about 50 h. The reduction of curvature of the beam is due to the swelling across the exposed surface of the adhesive. Beyond this exposure time, the bi-material curved beam warped and twisted. It is suggested that the warping and twisting are due to the non-uniform swelling and random degradation at the interface that produce an unbalanced shear stress that is responsible for the twisting.

Following the modelling of the curved beam in the previous section, a swelling analysis was implemented using the same FE model which included the moisture-dependent mechanical properties. This model was used to predict the reduction of the deflection of the curved beam. First, the curing process of the curved beam was modelled where it experienced a −70°C change in temperature. This predicted a deflection of about 4.8 mm before exposure to the moisture. Then, on exposure, moisture diffused into the adhesive layer. The diffusion was modelled using dual stage uptake model with diffusion parameters listed in Table 2 for a 2.0 mm thick adhesive film exposed to 95.8% RH at 50°C. After the diffusion analysis had been performed for a range of exposure times, the moisture concentration profiles obtained were read into the stress analysis as a predefined field variable. This changed the mechanical property of the adhesive. Then, the moisture concentration profiles were read in as a "temperature" field that caused swelling. The analysis was carried out for different exposure times and the change in the curved beam deflection was recorded. This high swelling at the exposed face changed the stress distribution and led to a reduction of the curvature. The T_g of the adhesive will be reduced with increasing moisture uptake. This was measured for a sample of the adhesive that was completely saturated and was found to be around 70°C. This is only 20°C above the temperature at which the exposure took place and thus the analysis might not fully represent the experimental conditions. Further research is being undertaken to investigate other effects, such as creep, on the predicted response.

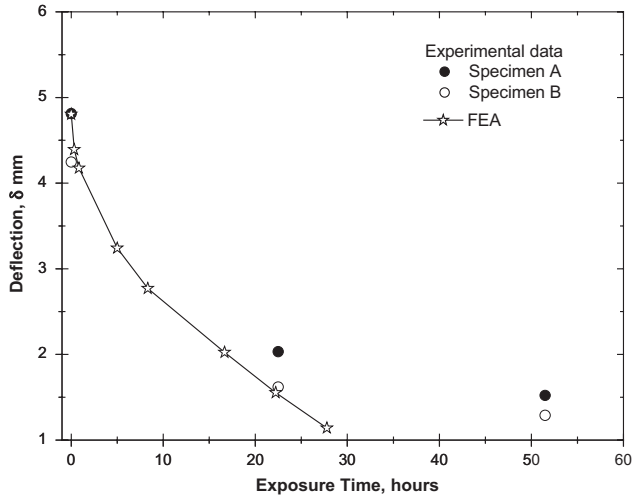

Fig. 17. Reduction in the deflection of the curved beam after exposure to moisture.

The analysis results in Fig. 17 show that the reductions of the curvature agree very well at the beginning but then the prediction deviates from experimental data after 25 h of exposure. The reason for this deviation was due to warping of the curved beam. The swelling coefficient and thermal expansion coefficient used gave excellent predictions even though they were obtained from separate experiments. This validated the reliability of the data and the techniques developed to measure them.

8. Conclusions

The work presented covers experimental work and complex coupled durability modelling in the moisture, thermal and stress domains. Gravimetric experiments were carried out to obtain the diffusion parameters of the adhesive. The results showed that the saturation level increased with increasing relative humidity. Fickian diffusion failed to model the uptake response of the bulk adhesive for all ageing environments and thicknesses. Instead, a dual stage uptake model has been proposed. This gave an excellent fit to the experimental results in all cases. The uptake of the thin specimens behaved more like the dual stage model whereas the thick specimens tended to approach a standard Fickian

response. A possible explanation for the dual stage process noted in the thinner specimens was given. This dual stage uptake process can be easily modelled using two separate standard Fickian diffusion FE analyses.

The swelling of the adhesive exhibited an approximately linear relationship with fractional mass uptake in the three different ageing environments studied, namely 81.2%, 95.8% RH and water immersion. The low swelling during initial moisture uptake is attributed to the ingress of moisture filling up the existing space with limited volumetric displacement. The prediction of the swelling response using a moisture-dependent swelling coefficient showed excellent results.

The bi-material curved beam experiment was used to determine the CTE of the AV119 adhesive. Further use of the bi-material curved beam was to investigate the interaction of thermal and swelling strains. The results showed the swelling of the adhesive reduces the curvature of the beams. However, when the swelling continues, warping of the specimen was noted. The reduction of the curvature when exposure to moisture was predicted excellently using the CTE, swelling coefficient and coupled moisture diffusion and stress analysis.

Acknowledgements

The authors would like to acknowledge EPSRC, Instron and DERA for their support of this work through grant GR/M92263. Special thanks go to Armourers & Brasiers' Company and Institute of Materials for providing conference travel grant support.

References

[1] Kinloch AJ. Durability of structural adhesives. Amsterdam: Elsevier Applied Science; 1983. p. 31 (ISBN 0853342148).
[2] Kinloch AJ. Adhesion and adhesives. London: Chapman & Hall; 1995 (ISBN 041227440X).
[3] Rowland SP. Water in polymers. ACS Symposium Series 127, 1979 (ISBN 0841205590).
[4] Rodriguez F. Principle of polymer systems, 4th ed. London: Taylor & Francis; 1996 (ISBN 1560323256).
[5] Crank J. The mathematics of diffusion, 2nd ed. Oxford: Oxford Science Publications; 1975 (ISBN 0198534116).
[6] Althof W. DFVLR-FB 79-06, 1979, RAE Translation 2038, 1979.
[7] Zhou J, Luca JP. Polymer 1999;40:5505–12.
[8] Zhou J, Lucas JP. Compos Sci Technol 1995;53:57–64.
[9] Roy S, Xu WQ, Park SJ, Liechti KM. Polym Polym Compos 2000;8:295–305.
[10] Hambly HO, Pan J, Crocombe AD, Megalis P. Euradh '96 1996;1:281–6.
[11] Brewis DM, Comyn J, Tredwell ST. Int J Adhes Adhes 1987; 7:30–2.
[12] Cai LW, Weitsman Y. J Compos Mater 1994;28:131–57.
[13] Gurtin ME, Yatomi C. J Compos Mater 1979;13:126–30.
[14] Carter HG, Kibler K. J Compos Mater 1978;12:118–31.
[15] Adamson MJ. J Mater Sci 1980;15:1736–45.
[16] El-Sa'ad L, Darby MI, Yates B. J Mater Sci 1989;24:1653–9.
[17] Chang T, Lai YH, Shephard NE, Sproat EA, Dillard DA. J Adhes 1997;60:153–62.
[18] Humfeld GR, Dillard Jr DA. J Adhes 1998;65:277–306.
[19] Nakano Y, Katsuo M, Kawawaki M, Sawa T. J Adhes 1998;65:57–80.
[20] Brewis DM, Comyn J, Raval AK, Kinloch AJ. Int J Adhes Adhes 1990;10:247–53.
[21] Wright WW. Composite 1981;12:201–5.
[22] Abdel Wahab MM, Crocombe AD, Beevers A, Ebtehaj K. Int J Adhes Adhes 2002;22:61–73.